

## Twist parameter Influence on Heat Transfer Coefficient Augmentation for a square Twisted Tube

Dr.Abdulkareem Abbas KhudhairAl-Musawi

Mechanical Engineering Department, University of Technology/ Baghdad

Email:karimmosawi@yahoo.com

Received on: 7/10/2012 & Accepted on: 31/1/2013

### ABSTRACT

Heat transfer augmentation due to twisting parameter was investigated in a twisted tube of square cross sectional area. Twisting parameter is defined as the ratio of the length of the tube where it completed twisting of 360 degrees to its hydraulic diameter.

Four twist parameters were chosen; 5, 10, 25 and 50, and a comparison is made with a straight untwisted duct.

Two sets of Reynolds numbers were considered for laminar and transient flow. The laminar flow is performed at  $Re = 500, 1000, 1500$  and  $2000$ . While for transient flow the range of Reynolds number are  $Re = 5000, 6000, 7000, 8000$  and  $9000$ . The influence of twist parameter on convective heat transfer coefficient in laminar and transient flow was investigated.

Numerical simulations were performed for three-dimensional, steady state incompressible flow in body-fitted coordinate using finite volume method and standard  $k - \epsilon$  turbulence model. For the heat transfer problem the uniform wall temperature (UWT) boundary condition at tube wall is considered.

It was observed that the heat transfer coefficient increases with decreasing twist parameter. This is interpreted to the nature of span wise swirling flow generated. The swirling increases cross flow velocity vectors as it becomes far from tube center towards walls. At tube wall the thickness of boundary layer becomes thinner as near wall velocity become larger which leads to a boundary layer of good thermal characteristics. Also swirling increases internal mixing process which enhances internal thermal equilibrium. The heat transfer coefficient also increases as Reynolds number increased as velocity components are increased.

**Keywords:** Heat transfer augmentation; Twisted tube; Twisting parameter.

تأثير عامل الالتواء على زيادة معامل انتقال الحرارة لأنبوب ملتوي مربع المقطع

الخلاصة

تمت دراسة زيادة انتقال الحرارة بسبب عامل الالتواء لأنبوب ملتوي ذو مقطع مربع. يعرف عامل الالتواء بأنه النسبة بين طول الأنبوب الذي يلتوي بزوايا قدرها 360 درجة إلى قطره

الهيدروليكي. وقد تم اختيار اربعة معاملات التواء و هي 5، 10، 25، 50 واجريت المقارنة مع انبوب غير ملتوي. تمت دراسة مجموعتان من اعداد رينولدز للجريان الطبقي و الانتقالي. حيث تم اختيار اعداد رينولدز 500، 1000، 1500، 2000 للجريان الطبقي. اما بالنسبة للجريان الانتقالي فقد تم اختيار اعداد رينولدز 5000، 6000، 7000، 8000 و 9000. لقد تمت دراسة تأثير عامل الالتواء على معامل انتقال الحرارة بالحمل في الجريان الطبقي و الانتقالي. تم اجراء المحاكات العددية لجريان ثلاثي الابعاد، مستقر، غير انضغاطي بالإحداثيات المطابقة للجسم بطريقة الحجم المحدد باستخدام نموذج الاضطراب  $k - \epsilon$  القياسي. و تم افتراض انتظام درجة حرارة الجدران كشرط حدي عند دراسة انتقال الحرارة. لوحظ ان معامل انتقال الحرارة يزداد مع ازدياد عامل الالتواء. وهذا ينسب الى طبيعة الجريان الدوامي المستعرض المتولد. حيث يزيد التدويم متجهات سرعة الجريان العرضية كلما ابتعدت عن مركز الأنبوب باتجاه الجدران. ان معامل انتقال الحرارة يزداد مع ازدياد عامل الالتواء. وهذا ينسب الى طبيعة الجريان الدوامي المستعرض المتولد. حيث يزيد التدويم متجهات سرعة الجريان العرضية كلما ابتعدت عن مركز الأنبوب باتجاه الجدران. عند الجدران تصبح سماكة الطبقة المتاخمة انحف كلما اصبحت السرعة قرب الجدار اعلى وهذا يحسن الخواص الحرارية للطبقة المتاخمة. كذلك التدويم يزيد من الخلط الداخلي الذي بدوره يعزز الاتزان الحراري. كذلك يزداد معامل انتقال الحرارة بزيادة رقم رينولدز كنتيجة لازدياد مركبات السرعة.

## INTRODUCTION

Heat transfer augmentation is the process of improving the performance of a heat transfer system by increasing the heat transfer coefficient. In the past decades, heat transfer enhancement technology has been developed and widely applied to heat exchanger applications in attempts to increase effectiveness and decreasing cost and size.

A variety of methods are implemented in order to do so, they are in general classified as active or passive methods. Passive methods require no extra power to enhance heat transfer by implementing, for example, surface roughness, surface pin fins, turbulence promoters, twisting tapes...etc. Active methods do need extra power, for example mixing mechanism, the injecting or imparting a tangential flow. Passive methods are more preferable and are widely used.

The general way to augment heat transfer coefficient is to:

- Increasing mixing process.
- Thinning boundary layer thickness.
- Increasing gradients at near wall region.

Utilizing twisting tubes in heat exchangers is a promising technique which achieved the above three enhancement parameters and it is a passive method. The Twisted Tube heat exchanger originated in Eastern Europe and became commercially available in the mid of eighteens. It was developed primarily to overcome the limitations inherent with conventional shell and tube technology [1]. Apart from the enhancement consideration, the present study was also motivated by the need in understanding the heat transfer mechanism of gas turbine blade cooling process. The cooling channel of a gas turbine is often modeled by a duct with a square cross section [2].

Although works concerning flow patterns in twisted square ducts are available but unfortunately literatures related to heat transfer coefficient investigation is very limited in public. Masliyah and Nandakumar [3] numerically studied the fully

developed steady laminar flow through twisted square ducts with a rotation coordinate system. Axial conduction in fluids was neglected to preserve the two-dimensional nature of the problem. Temperature along the periphery was assumed to be constant for each wall, but it might be different for four walls. It was observed that in the Reynolds number range between 1–1000 and a dimensionless twisting parameter of 2.5, swirling motion provides significant enhancement in overall heat transfer. Liang-Bi Wang and his colleagues [5], conducted an experimental and numerical study of turbulent heat transfer in twisted square ducts. They investigated heat transfer coefficient in three types of twisted tube, twisted uniform cross section square duct, twisted divergent square duct and twisted convergent square duct. The twisting parameter was taken as 42. Both experimental and numerical results show that the twisting brings about a special variation pattern of the span-wise distribution of the local heat transfer coefficient, while the divergent and convergent shapes lead to different axial local heat transfer distributions. Based on the test data, the thermal performance comparisons were made under three constraints (identical mass flow rate, identical pumping power and identical pressure drop) with straight untwisted square duct as a reference. Comparisons showed that the twisted divergent duct can always enhance heat transfer, the twisted convergent duct always deteriorates heat transfer, and the twisted constant cross section duct is somewhat in between. Blazo Ljubcic[6] describes testing of an advanced shell-and-tube design with twisted tubes for several configurations. Its performance has been tested under single-phase, fully developed, transition flow conditions. Each test examining heat transfer and pressure drop for the particular heat exchanger. It was shown that overall heat transfer and pressure drop increased with a smaller tube twist pitch to diameter ratio, and that these exchangers have specific advantages and characteristics, previously known only to plate exchanger users. Twisted tubes increase the level of mixing and promote turbulence in the low Reynolds number range, on both, tube-side and shell-side of the tubes.

In this study the influence of twisting parameter on convective heat transfer coefficient in twisted tubes for, fully developed, laminar and transition flow was investigated numerically to demonstrate the augmentation of heat transfer due to twisting.

**MATHEMATICAL MODELING**

The case was handled mathematically by assuming that the flow is three-dimensional, steady state, incompressible flow. The following general partial differential, time averaged, governing equations in Cartesian coordinate system for incompressible flow are solved in body fitted coordinate system:

Continuity equation:

$$div \vec{q} = 0 \quad \dots (1)$$

Conservation of momentum:

$$\rho \, div(\phi \cdot \vec{q}) = -grad \, p + \Gamma_\phi \, div (grad \, \phi) + S_\phi \quad \dots (2)$$

$$\vec{q} = ui + vj + wk$$

Where  $\vec{\phi}$  stands for Cartesian velocity components and  $S_\phi$  stands for  $S_x$ ,  $S_y$ , and  $S_z$  which are source terms due body force and they are equal zero for the case under consideration.  $\Gamma_\phi$  is effective diffusion parameter due to viscosity. The effective viscosity is defined as:

$$\mu_{eff} = \mu + \mu_t \quad \dots (3)$$

Conservation of energy:

$$\rho \operatorname{div}(T \cdot \vec{q}) = \Gamma_T \operatorname{div}(\operatorname{grad} T) + S_T \quad \dots (4)$$

The source term  $S_T$  is due to heat source which is zero for the case under consideration, and the diffusion parameter:

$$\Gamma_T = \frac{k}{c} = \Gamma_l + \Gamma_t = \frac{\mu}{\sigma_l} + \frac{\mu_t}{\sigma_t} \quad \dots (5)$$

In this equation  $k$  is the conductivity and  $C$  is the specific heat and  $\sigma_l$  and  $\sigma_t$  are laminar and turbulent Prandtl number.

Although the laminar or molecular viscosity ( $\mu$ ) is temperature dependent, it is assumed constant, since the variation in its value with range of temperatures under consideration is small. The turbulent or eddy viscosity ( $\mu_t$ ) is evaluated after solving a relevant turbulence model. The turbulent Prandtl number  $\sigma_t = Pr_t$  value is (0.7 to 0.9), which is usually taken 0.9 [8] while the laminar Prandtl number  $\sigma_l$  is calculate from  $\sigma_l = Pr_l = \nu/\alpha = \mu c/k$ , where  $\alpha = k/\rho c$ .

The standard ( $k - \epsilon$ ) turbulence model is chosen for its simplicity, [8], to model turbulent kinetic energy  $k$  and turbulent kinetic energy dissipation  $\epsilon$ .

$$\rho \operatorname{div}(k \cdot \vec{q}) = \operatorname{div}(\Gamma_k \operatorname{grad} k) + S_k \quad \dots (6)$$

$$\rho \operatorname{div}(T \cdot \vec{q}) = \operatorname{div}(\Gamma_\epsilon \operatorname{grad} \epsilon) + S_\epsilon \quad \dots (7)$$

The eddy viscosity is evaluate from Prandtl-Kolmogorov relation

$$\mu_t = \rho * C_\mu * \frac{k^2}{\epsilon} \quad \dots (8)$$

The constants values for ( $k - \epsilon$ ) turbulence model are taken as in refs [7, 8].

### TRANSFORMATION

All equations in Cartesian coordinate were transferred into a body fitted coordinate system. Details of transformation for continuity, momentum and turbulence model can be found in refs [9]. The detailed transformation of energy equation is lengthy but generally is similar to the transformation of momentum equations. The final transformation for the energy equation is:

$$(\rho UT)_\zeta + (\rho VT)_\eta + (\rho WT)_\xi = (J\Gamma_T T_\zeta \alpha 1)_\zeta + (J\Gamma_T T_\eta \alpha 2)_\eta + (J\Gamma_T T_\xi \alpha 3)_\xi + S_T \dots (9)$$

The value of source term  $S_T$  is zero for all internal nodes, except near walls, since there is no internal heat generation. The diffusion parameter  $\Gamma_T$  is the same as mentioned in eq. 5.

**DIFFERENCING AND DISCRETIZATION**

All equations of a form similar to equation (9) were differenced and discretized to equations of a form similar to the following algebraic linear equation

$$A_P T_P = A_E T_E + A_W T_W + A_N T_N + A_S T_S + A_F T_F + A_B T_B + b \dots (10)$$

Details of differencing and discretization in general are nearly similar as for the momentum equations [9] with some reservation. A set of algebraic linear equations for the variables  $U, V, W, k, \epsilon$  and  $T$  for each internal node is solved to calculate Cartesian velocity, pressure and temperature field. A segregate, staggered technique is used similar to the SIMPLE algorithm recommended by Patanker, S. [10].

When the solution is converge, temperature is found, the local and total Nusselt number are then evaluated.

**HEAT TRANSFER COEFFICIENT**

From energy balance for the control volume shown in Figure (1), at any section of unit width, the net of heat increase (or decrease) through the control volume is equal to the heat convection into (or out of) the control volume. The heat convection from internal fluid to wall is equal to the heat conducted towards wall through boundary layer adjusted to it as the velocity goes to rest and gradients become high.

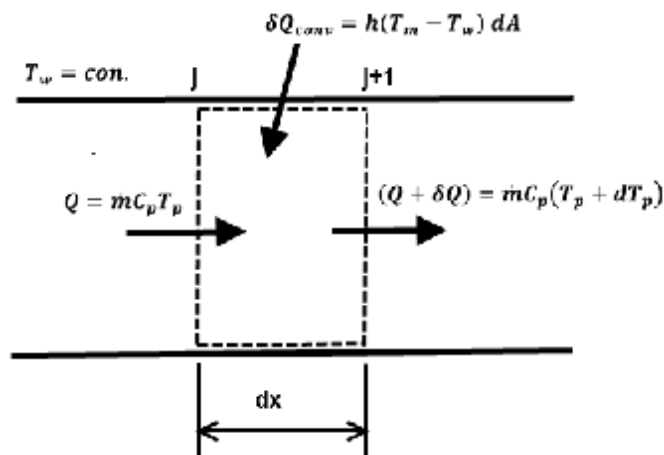


**Figure (1) Sectional Control Volume.**

$$\delta Q_{conv} = h(T_m - T_w) dA \quad \dots (11)$$

$$\delta Q_{C.V.} = \dot{m}C_p dT_b \quad \dots (12)$$

The local convection heat transfer coefficient and Nusselt number are evaluated with respect to sectional bulk temperature  $T_{b,j}$ . As the temperature field can be evaluated numerically, the local Nusselt was evaluated as follow;

$$h_x(T_w - T_m)dA_s = \dot{m}C_p dT_b \quad \dots (13)$$

$$h_x = \frac{\rho u_m A_{cross} C_p (T_{b,j+1} - T_{b,j})}{A_s (T_w - T_m)} \quad \dots (14)$$

$$T_{m,j} = \frac{(T_{b,j+1} + T_{b,j})}{2} \quad \dots (15)$$

For constant wall temperature where  $dT_m = -d(T_w - T_m)$  and mean bulk temperature  $dT_m$  is approximate by bulk temperature  $dT_b$ .

$$h_x dA_s = \dot{m}C_p \frac{dT_b}{(T_w - T_b)} \quad \dots (16)$$

$$h_x = \frac{\rho u_m A_{cross} C_p}{A_s} \ln \frac{(T_{b,j+1} - T_w)}{(T_{b,j} - T_w)} \quad \dots (17)$$

$$N_{u,local} = \frac{h_x D_x}{k} \quad \dots (18)$$

At each section along the tube, from  $j = 2$  to  $j = NJ - 1$ , the frontal area of each cell is define as:

$$Cell\ area, A_{i,j} = |r_\zeta \times r_\xi| = \sqrt{|r_\zeta^2||r_\xi^2| - |r_\zeta \cdot r_\xi|^2} \quad \dots (19)$$

$NJ$  is the number of cells along the longitudinal tube direction ( $\eta$ ) and  $j$  is a counter in this direction and here  $r_\zeta$  and  $r_\xi$  are vector position tangent to  $\zeta$  and  $\xi$  cross wise coordinate lines.

The mean temperature at each section is evaluated from conservation of energy, i.e.

$$T_{b,j} = \frac{\int C_p T_{i,k} \delta \dot{m}}{\dot{m} C_p} = \frac{\rho C_p \sum T_{i,k} vel_{i,j} A_{i,k}}{\rho C_p \sum vel_{i,j} A_{i,k}} = \frac{\sum T_{i,k} vel_{i,j} A_{i,k}}{u_m A_{sec}} \quad \dots (20)$$

Where:  $vel_{i,j}$  is the velocity component perpendicular to cell area  $A_{i,k}$  along main stream wise direction. For twisted or curved tubes vector mathematics is utilized to evaluate this velocity but the covariant velocity component along  $\eta$  (stream-wise coordinate) is quite sufficient, while for straight tubes this velocity is identical to the Cartesian velocity component along the tube (y-coordinate).

The overall convection heat transfer coefficient and Nusselt number are evaluated as:

$$h_{overall} = \frac{1}{NJ - 2} \sum_{j=2}^{j=NJ-1} h_{local} \quad \dots (21)$$

$$Nu_{overall} = \frac{1}{NJ - 2} \sum_{j=2}^{j=NJ-1} Nu_{local} \quad \dots (22)$$

**NEAR WALL TREATMENT**

The internal duct flow becomes turbulent, in general, at  $Re \geq 10^4$ , while it is laminar at  $Re \leq 2000$  [12], and the transition region is between. Due to the swirling nature for twisted tubes the flow is expected to be turbulent at earlier Reynolds number.

For laminar flow, a source term in momentum equations is arisen due to shearing force at near wall and details can be found in references [8,9]. For energy equation, the source term for eq. (9), ( $S_T$ ), is introduced as follow; a conduction heat transfer per unit volume comes into (or out) the near wall cell as:

$$q_s = -k \frac{\Delta T}{y_p} = -k \frac{T_p - T_w}{y_p} A_{s,cell} \quad \dots (23)$$

$$S_T = S_u + S_p T_p$$

$$S_u = k \frac{T_w}{y_p} A_{s,cell} \quad ; \quad S_p = -\frac{k}{y_p} A_{s,cell} \quad \dots (24)$$

$$b = -\frac{k}{y_p} A_{s,cell} \cdot T_p + k \frac{T_w}{y_p} A_{s,cell} \quad \dots (25)$$

The term  $S_p = -k/y_p A_{s,cell}$  must be transferred the left hand side of eq. (10) to enhance the convergence of the solution [10]. Eq. (10) becomes.

$$(A_p + S_p) T_p = \sum (A T)_{neighbor} + S_u \quad \dots (26)$$

For turbulent flow the near wall nodes could lie in a viscous sub layer or turbulent region. If the near wall node lies in a region where ( $y^+ \leq 11.63$ ), then the flow obeys the viscous relation. Reynolds stresses are ignored and the node is considered a solid boundary for the solution of ( $k - \epsilon$ ) equations, i.e. ( $k_p = 0$ ), ( $\epsilon_p = 0$ ) and ( $\mu_t = 0$ ). The relations for laminar flow are prevailed.

If the value of ( $y^+ > 11.63$ ), the near wall node is assumed to lie in a log-law region where then the flow is considered fully turbulent. The Reynolds stresses are dominant [7,8]. Manipulation the source term for momentum and ( $k - \epsilon$ ) model was found in reference [7, 8 and 9].

For energy equation, the following treatment is adapted [7,8]:

$$q_w = - \frac{\rho C C_\mu^{1/4} \sqrt{k_p} (T_p - T_w)}{T^+} A_{s,cell} \quad \dots (27)$$

$$S_p = - \frac{\rho C C_\mu^{1/4} \sqrt{k_p}}{T^+} A_{s,cell} \quad \dots (28a)$$

$$S_u = \frac{\rho C C_\mu^{1/4} \sqrt{k_p} T_w}{T^+} A_{s,cell} \quad \dots (28b)$$

$$T^+ = - \frac{\rho C u_\tau (T_p - T_w)}{q_w} = \sigma_{T,t} (u^+ + Pee) \quad \dots (29)$$

$$pee = 9.24 [(\sigma_l / \sigma_t)^{0.75} - 1] \{1 + 0.28 \exp[-0.007(\sigma_l / \sigma_t)]\} \quad \dots (30)$$

$$u_\tau = (\tau_w / \rho)^{1/2} \quad \dots (31)$$

$$u^+ = u / u_\tau = \frac{1}{\kappa} \ln E y^+ \quad \dots (32)$$

Where  $\kappa = 0.4187$  is Von Karman's constant,  $E = 9.8$  is Wall roughness parameter and  $C_\mu = 0.09$  is a constant.

#### BOUNDARY CONDITION

At inlet Dirichlet b.c. was assumed. Velocities are  $v_{in} = const$ ,  $u_{in} = 0$ ,  $w_{in} = 0$ ,  $p_{in} = const$  and  $p_{in} = const$ . Turbulence level is taken as [5]  $k_{in} = a_k * u_m^2 / 2$ , where  $a_k = 0.005 - 0.015$  and  $\epsilon_{in} = \sqrt[3]{k^2} / 0.05 D_h$ .

At wall no slip condition was imposed at walls, i.e.  $u_{wall} = 0$ ,  $v_{wall} = 0$  and  $w_{wall} = 0$ . a constant temperate distribution was assumed. A Neumann b.c was assumed for pressure i.e.  $\partial p / \partial n = 0$ .

Dirichlet b.c. was assumed for turbulence parameters a, i.e.  $k_{wall} = 0$  and  $\epsilon_{wall} = 0$ .

At exit a zero gradient condition (Neumann b.c) for all variables was imposed.

A set of equations similar to eq. (26) for  $(u, v, w, p \text{ and } T)$  at each node within the domain are solved by SIMPLE method in a BFC system.

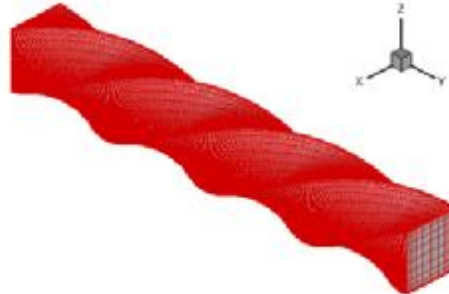


**Figure (2) wisted Tube.**

### **TUBE GEOMETRICAL CHARACTERISTICS**

The tube geometry under consideration is a straight twisted uniformly with square cross section area of  $50 \text{ mm} * 50 \text{ mm}$ . The ratio of the tube length to its hydraulic diameter to complete twisting of 360 degrees ( $s/d$ ) is a dimensionless twisted parameter. Four twisted parameters of 5, 10, 25 and 50 were considered, see Figure (2). The twisted tube length is  $100D_h$  for laminar flow. For transient flow, the twisted tube length is  $200D_h$ . This length is quite sufficient to ensure that the flow at exit is fully developed and also to ensure that the solution is affected mainly by the inlet and walls b.c. only.

Number of grids along the tube is  $11 * 501 * 11$ . The comparison for laminar flow was conducted at Reynolds numbers 500, 1000, 1500 and 2000. For transient flow, the comparison is conducted at Reynolds 5000, 6000, 7000, 8000 and 9000. The comparison is also performed with a straight tube with the same geometry.

### **GRID GENERATION**

Since the tube cross section is square and the twist is linear, then a kind of direct method is used to generate grids with relevant stretching parameters to cluster grids towards wall in order to capture wall main variables gradients [13].

### **CODE CONSTRUCTION**

The code is constructed in a Fortran-90 language. It is a modified version constructed by the author where the energy equation is newly manipulating and introduced in the code. The code implements the BFCS where each partial in the Cartesian coordinate gives three partials multiply by their transformation Metres which increases processing time and computer accumulating errors. So some discrepancy during verification is expected. Nevertheless the Body Fitted Coordinate System is a default with problem under consideration, i.e. twisted tubes.

**VALIDATION**

To validate the heat transfer coefficient calculation, for fully developed flow, a plain tube with the same diameter and length was used and the results were compared with published data.

Two cases were considered for plain square duct.

- Case I: Laminar flow at  $Re=1000$ . Figure (3) shows the comparison of forced local Nusselt number distribution predict by the present work with the data presented by Mujumdar for square tube [14]. The agreement is found good for both data.
- Case II: Turbulent flow at  $Re=10000$ . Figure (4) shows the predicted Nusselt number distribution. At fully developed flow the average Nusselt is  $Nu = 39$  which is closed to the value  $Nu = 41$  predicted by Rivas G.A. [15]. According to Dittus–Boelter equation for circular tubes [16],  $Nu = 33$ , which means that the empirical formula for circular cross section tubes cannot predict Nusselt number in square ducts correctly.

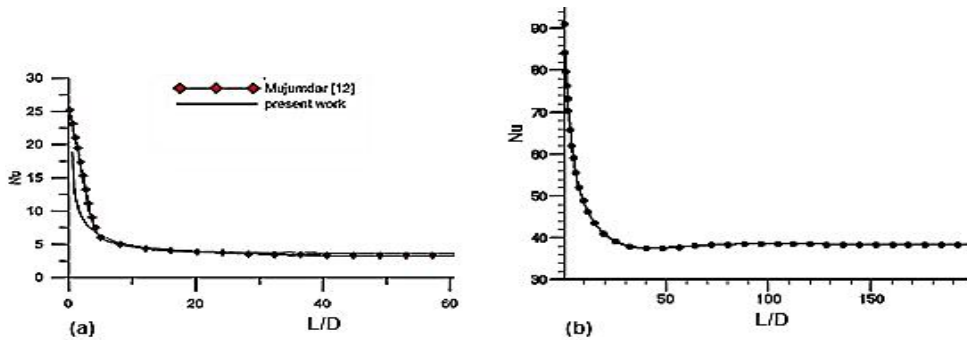


Figure (3): Nusselt Number Distribution for Fully Developed Flow at  
a)  $Re = 1000$  b)  $Re = 10000$

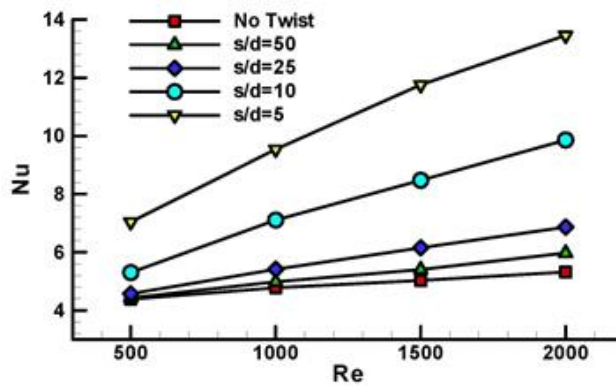


Figure (4): Nusselt number vs. Reynolds number at different twist parameters for laminar flow

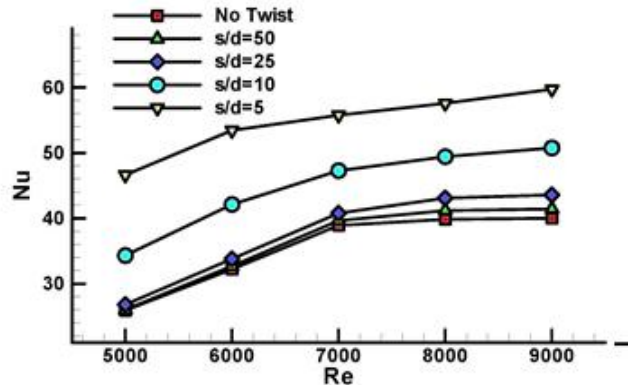


Figure (5): Nusselt number vs. Reynolds number at different twist parameters for transient flow

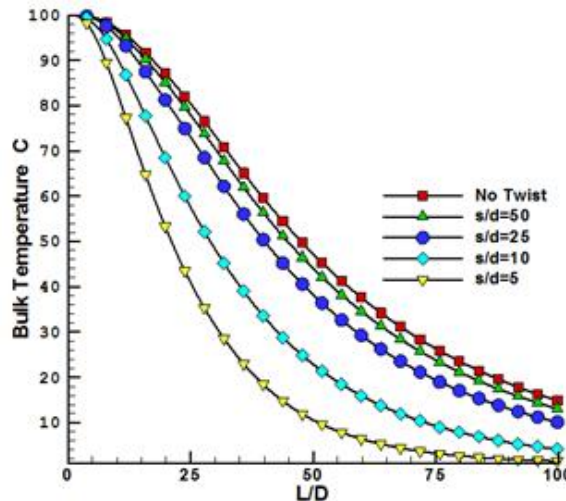


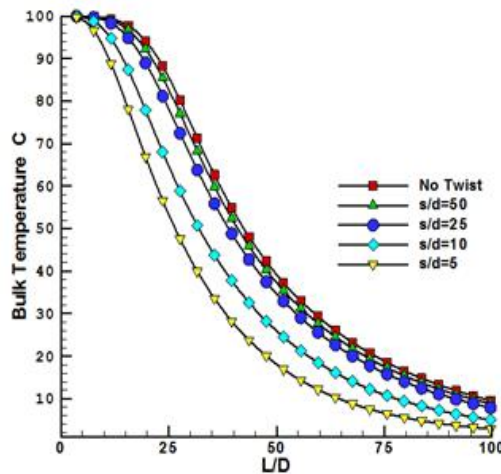
Figure (6) The bulk temperature distribution at Reynolds numbers for laminar flow at Re= 1000

**RESULTS AND DISCUSSION**

Figure (4) represents the variation of Nusselt number with Reynolds number for different twist parameters for laminar flow. It is obvious that the enhancement of Nusselt with twist is clear. This is due to the fact that the twist in such polygonal tubes creates transverse flows and the absolute velocity near wall becomes larger and consequently the gradient becomes larger. Then transportation of heat is increased as fluid momentum near wall is increased since velocities are responsible for the convection of momentum which is a major part in momentum equation, eq (2). Also the rotating nature of flow within the twisted tube creates centrifugal force pushing lumps of fluids towards the wall and these relatively high radial

momentum lumps exchange position with these adjacent to the wall. Due to the fore-mentioned facts the boundary layer is thinning and its thermal resisting is reduced. The three types of motions, longitudinal, traverse and radial, provoke fluid mixing plus thin boundary layer and high gradients adjacent to the wall enhancing heat exchange with walls and the result is a high convection heat transfer. Particles is started due to the inception of turbulent eddies. As the twist parameter increases the inception of turbulence starts at earlier Reynolds number since twist acts as turbulence agitation.

Figure (5) represents the variation of Nusselt number values for different twist parameters with Reynolds number at transient flow. It shows similar trends. The increase of Nusselt number twist parameter is significant since mixing within the fluid. Figure (6) represent the tube-wise bulk temperature distribution at Reynolds numbers 1000. For laminar flow the influence of twist parameter is obvious. The bulk temperature degraded faster as the twist parameter increased since twisting



increases mixing characteristics.

**Figure 7: The bulk temperature distribution at Reynolds numbers for transient flow at Re= 7500**

Figure (7) represents the tube-wise bulk temperature distribution at Reynolds numbers d 7500. For transient flow the twist parameter has also a significant role in augmenting heat transfer convective coefficient as it clear from figure (8), but the role of turbulence in fluid mixing mechanism started strongly to take his part to enhance convective heat transfer.

**CONCLUSIONS**

The increasing in convective heat transfer coefficient due to twist parameter effect can be interpreted to:

1. Increasing internal thermal equilibrium due the internal mixing process by swirling.
2. Improving boundary layer thermal characteristics as it becomes thinner.
3. Increasing near wall velocity gradients.

Although The standard ( $k - \epsilon$ ) model recommended for general purpose CFD computations, but the  $\epsilon$  equation has long been suspected as one of the main sources of accuracy limitations for the standard version of the ( $k - \epsilon$ ) model [8] in flows that experience large rates of deformation. The Linear Eddy Viscosity Model (LEVM) ( $k - \epsilon$ ) can give rise to inaccurate predictions for the Reynolds normal stresses and so that it does not have the ability to predict secondary flows in non-circular ducts due to its isotropic nature. In spite of that, they are one of the most popular models in the engineering due to its simplicity, good numerical stability and it can be applied to a wide variety of flows.

For the present study this (LEVM) ( $k - \epsilon$ ) model does not predict reasonably the thermal issues for flow of  $Re > 10^4$ . In future the intention is to extend this study for turbulent flow of  $Re > 10^4$  by implementation of a more relevant turbulence model such as the Nonlinear Eddy Viscosity Model (NLEVM) the variants of the ( $k - \epsilon$ ) model or the Reynolds Stress Model (RSM), The (RSM) model has shown superiority regarding the models of two equations in complex flows that involve swirl, rotation, etc. [15]. However the implementation of RSM model in a BFC system is a major task.

#### REFERENCES

- [1]. Donald Morgan, R. "Twisted tube heat exchanger technology", Brown Fintube Company, 2010.  
E-mail: [morganOd@kochind.com](mailto:morganOd@kochind.com).
- [2]. Han, J. C., Zhang, Y. M., Lee, C. P., "Augmented Heat Transfer in Square Channels with Parallel, Crosses, and V-Shaped Angled Ribs," ASME. J. Heat Transfer, 113, pp. 590–596, 1991.
- [3]. Masliyah, J. H., and Nandakumar, K., "Steady Laminar Flow through Twisted Pipes: Fluid Flow in Square Tubes", ASME J. Heat Transfer, 103, pp. 785–790, 1981.
- [4]. Masliyah, J. H., and Nandakumar, K., "Steady Laminar Flow through Twisted Pipes: Heat Transfer in Square Tubes", ASME J. Heat Transfer, 103, pp. 791–796, 1981.
- [5]. Liang-Bi Wang, Wen-Quan Tao, Qiu-Wang Wang and Ya-Ling He, "Experimental and Numerical Study of Turbulent Heat Transfer in Twisted Square Ducts", ASME J. of Heat Transfer, 123, pp. 868-877, 2001.
- [6]. Blazo Ljubicic, "Testing of Twisted-Tube Exchangers in Transition Flow Regime", Brown Fintube Company, Koch Industries,  
E-mail: [ljubicb@kochind.com](mailto:ljubicb@kochind.com).
- [7]. Awbi H. B., Ventilation of Building, E and FN Spon Inc, 1998.
- [8]. Versteeg H. K. and Malalasekera W., An Introduction to Computational Fluid Dynamics The Finite Volume Method, Longman Group Ltd, 1995.
- [9]. Khudhair, A. K. A., "Computational Fluid Dynamics with Practical Reference to Centrifugal Pump Impellers", Ph.D. thesis, Mechanical Engineering Department, University of technology, 2003.
- [10]. Patankar, v. S., Numerical heat transfer, Hemisphere Publishing Corporation, 1980.

- [11]. Hongxing Yang, Tingyao Chen, Zuojin Zhu, "Numerical Study of Forced Turbulent Heat Convection in a Straight Square Duct", International Journal of Heat and Mass Transfer 52, 3128–3136, 2009.
- [12]. Yunus A. Cengel, Heat transfer, A practical approach, 2<sup>nd</sup> edition, 2003.
- [13]. Anderson, D. A., Tannell, J. C., and Pletcher, R. H., Computational Fluid Mechanics and Heat Transfer. Hemisphere publishing corporation, Taylor & Francis group, N. Y., 1984.
- [14]. Mujumdar, A. S. "Heat Transfer in Square Duct", University of Singapore, 2009.
- [15]. Rivas, G.A. E.C. Garcia, M. Assato, "Forced turbulent heat convection in a square duct with non-uniform wall temperature", International Communications in Heat and Mass Transfer 38, pp 844–851, 2011.
- [16]. Holman, J. P. Heat Transfer, 9<sup>th</sup> ed, Tata McGraw-Hill Publishing Company Limited, 2008.

#### NOMENCLATURE

- $A_{cross}, A_s$  : Tube cross area, surface strip area  
 $A_{s, cell}$  : Cell surface area  
 $C$  : Specific heat at constant pressure.  
 $D_h$  : Tube hydraulic diameter.  
 $h, k, \alpha$  : Heat transfer coefficient, Thermal conductivity and thermal diffusivity.  
 $k, \Gamma_k, S_k$  : Turbulent kinetic energy, diffusivity and source term  
 $n, y_p$  : Normal distance from near wall cell node to the wall.  
 $Nu, Pr_l, Pr_t$  : Nusselt, laminar and turbulent Prandtl numbers.  
 $P, C_p$  : Pressure and pressure coefficient.  
 $\bar{q}$  : Velocity vector  
 $q_w$  : Wall heat flux  
 $T, \Gamma_T, S_T$  : Temperature, thermal diffusivity and source term for energy equation.  
 $T_b, T_m, T_w$  : Bulk, mean and wall temperature.  
 $T^+$  : Universal near wall temperature distribution.  
 $u, \Gamma_x, S_x$  : Velocity, viscose diffusivity and source term in x-direction.  
 $u^+, u_\tau, u_m$  : Non-dimensional, wall tangential, Friction and mean velocity  
 $U, V, W$  : Contravariant velocity components  
 $v, \Gamma_y, S_y$  : Velocity, viscose diffusivity and source term in y-direction.  
 $w, \Gamma_z, S_z$  : Velocity, viscose diffusivity and source term in z-direction.  
 $\varepsilon, \Gamma_\varepsilon, S_\varepsilon$  : Kinetic energy dissipation, diffusivity and source term  
 $\tau_w$  : Wall shear stress

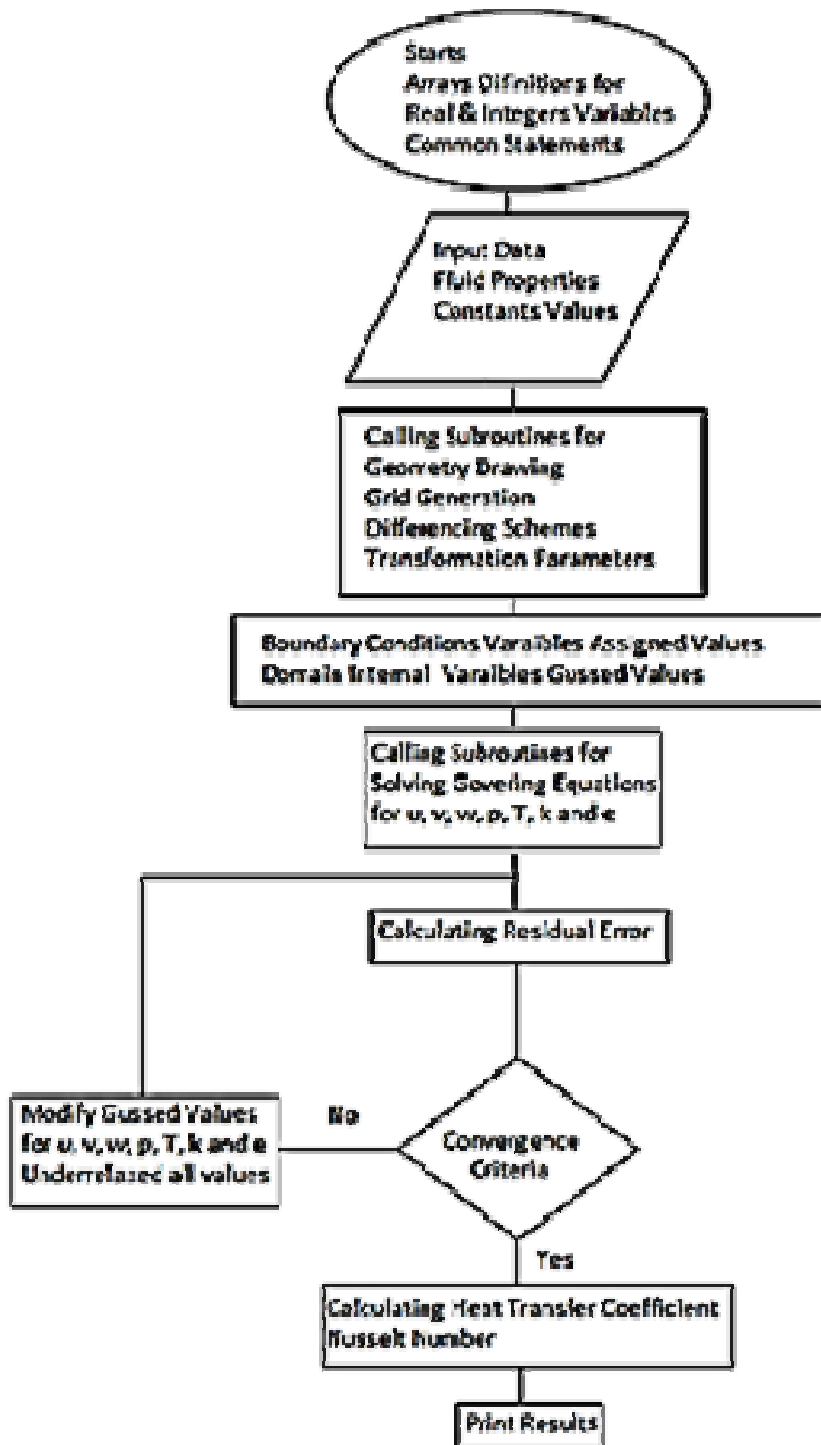


Figure 8: The Flow chart of the code developed